

## SITE-EFFECTS ESTIMATION AND SOURCE-SCALING DYNAMICS FOR LOCAL EARTHQUAKES AT MT. VESUVIUS, ITALY

Danilo Galluzzo<sup>1</sup>, Edoardo Del Pezzo<sup>1</sup>, Rosalba Maresca<sup>2</sup>, Mario La Rocca<sup>1</sup>,  
Mario Castellano<sup>1</sup>

*1 INGV – Osservatorio Vesuviano, Napoli, Italy*

*2 Università del Sannio, Benevento, Italy*

**ABSTRACT** - Local microearthquakes were used to estimate site effects and source dynamic-scaling characteristics at Mt. Vesuvius, Italy. The selected data set is composed of low magnitude events ( $1.1 \leq M_d \leq 3.6$ ) recorded in 1996 and 1999 by nine digital short-period (1-Hz) seismic stations. Site response was evaluated by analysing data with three different approaches: 1) spectral ratios method of S-waves with respect to the average amplitude spectrum; 2) generalized inversion for site and source from the S-waves; and 3) generalized inversion from the coda waves. The results obtained with all three methods showed amplification of a factor of 1.5-2.5 in the 8-14 Hz frequency band for BKE and SGV sites and an amplification of 3 in a narrow band around 8 Hz for the CDT site. Method 2 allowed simultaneous determination of the source spectral shape for each earthquake. By assuming an  $\omega^2$  source model, we estimated the seismic moment  $M_0$  and corner frequency  $f_c$ . The results show that most of the selected earthquakes are characterized by stress drops of 10 bars. The present results are encouraging for further investigation into the techniques for site-effect evaluation and for improving our knowledge of the scaling law of the source spectrum at Mt. Vesuvius.

### 1. Introduction

The Mt Vesuvius area is potentially one of the most dangerous volcanic areas in the world. This is due to the closeness of the volcano to a densely inhabited zone. The knowledge of the site-response function is one of the most critical factors for the estimation of seismic hazard and the determination of earthquake source parameters. The present study investigated the site-amplification effects in the Mt. Vesuvius area (Southern Italy) that can be inferred by data from local earthquakes.

The good quality of seismic data collected in the period from 1996-1999 has allowed us to evaluate the site effects using empirical approaches. We have evaluated the site amplification for the S-wave windows of seismic records using classical (direct) spectral ratios (DSR; Borchardt, 1970; Bonilla et al., 1996, Lachet et al., 1996; Del Pezzo et al., 1987), the generalized inversion (GI) method (Hartzell, 1992; Bonilla et al., 1996, Parolai et al., 2001, Drouet et al., 2005), and the coda inversion (CI) technique (Tsujiura, 1978; Bonilla et al., 1996). The first method is based on the ratio between the spectrum of the site of interest and the spectrum at a reference site, which is a nearby hard rock site. Here, the lack of a hard rock site led us to consider the average spectrum between all of the investigated sites as the reference spectrum. A similar assumption was made for the second method (GI technique of S-wave spectra). In this case, the average spectra evaluated at all of the stations is constrained at unity (Hartzell, 1992). By applying this last

method, we corrected the amplitude spectra for geometrical spreading and the quality factor  $Q$ . Due to the limited dataset available for the application of these first two methods (the difficulty in the identification of the S onset), we tried to use the radiation present in the late S coda, where the radiation pattern effects are averaged out to estimate the amplification factors of the investigated sites (Tsuijura, 1978; Bonilla et al., 1996; Lachet et al., 1996), and compared the results with the previous two methods. The aim was thus to compare the results of the site-transfer function for each site obtained with these three different methods. The comparison was made in terms of peak frequencies and relative amplitudes of the evaluated site-transfer functions. To evaluate the differences between the different methods, the uncertainties of each method were also calculated. As several studies have shown, the GI method for the S-wave can be successfully applied to isolate the source term from the spectra of the earthquake waveform (Jin et al., 2000; Parolai et al., 2001; Drouet et al., 2005). The joint inversion for the evaluation of site and source term gave us the possibility of evaluating the spectral parameters of the earthquake source (seismic moment, corner frequency and source dimension). The distribution of seismic moment versus the source dimension can have a key role in the validation of the self-similarity of earthquake distribution in the area under investigation.

## 2. Data Set

We analyzed short-period seismograms from 31 local earthquakes recorded by nine digital seismic stations deployed on Mt Vesuvius, in the years 1996 and 1999 (Fig. 1).

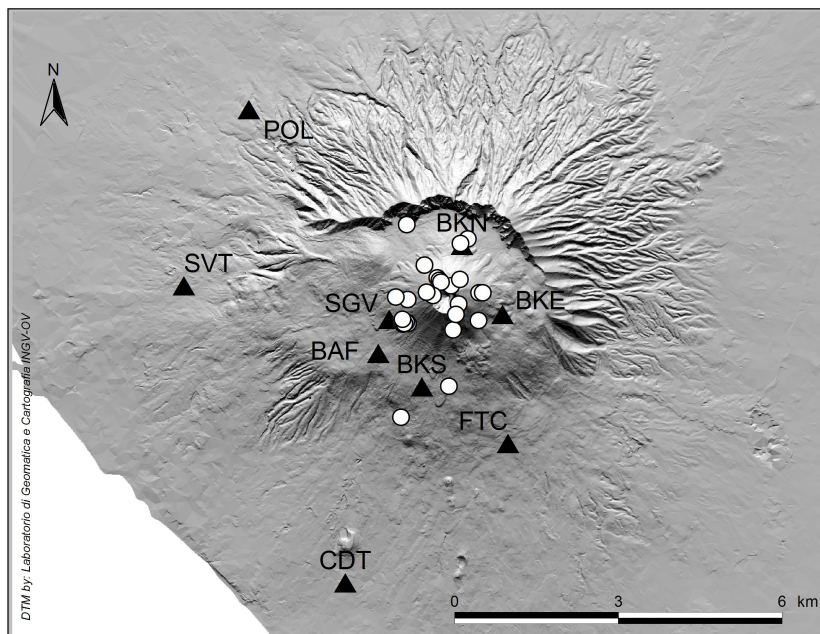


*Figure.1 – Map of the Mt. Vesuvius area. The recording sites and earthquakes epicenters are shown with black triangles and white circles, respectively.*

The data set was composed of low to moderate earthquakes ( $1.1 \leq M_d \leq 3.6$ ) located at depths between 0.0 km and 4.2 km b.s.l. The BKE, BAF, SGV, BKN and BKS digital stations were equipped with digital station PCM 5800 Lennartz with MARK L4C 3-

component sensors (1 Hz). The POL, SVT and CDT stations were equipped with MarsLite Lennartz stations with LE3Dlite 3-components sensors (1 Hz). The digital stations sampled seismic signals at 125 Hz, with a low-pass anti-alias filter at a cut-off frequency of 25 Hz. All of the available waveforms were corrected for instrument response.

### 3. Methods of analysis

#### 3.1 Direct Spectral Ratios

A seismogram can be represented in the frequency domain as the product of source, path, site effect and instrument response:

$$A_{ij}(f) = K_i(f) \cdot P_{ij}(f) \cdot S_j(f) \cdot I_j(f) \quad (1)$$

where  $K_i$  is the source term of the  $i$ th event,  $P_{ij}$  is the path term including the geometrical spreading and attenuation term between the  $i$ th event and  $j$ th station,  $S_j$  is the site term for the  $j$ th station and  $I_j$  is the instrument-response term for the  $j$ th station. The  $i$  and  $j$  indices are referred to the  $i$ th seismic event ( $i = 1 \dots n$ ) and  $j$ th site-station ( $j = 1 \dots N$ ), respectively. In the present study, the spectral amplitude  $A_{ij}(f)$  was obtained by considering the logarithmic average of the spectral amplitudes obtained on the north-south and east-west components. The window length for the S-wave window is fixed at 3 s after the picking of the S-wave arrival. If the attenuation parameters, travel times and instrument characteristics are known, the spectral amplitude  $A_{ij}(f)$  can be corrected for the  $P_{ij}(f)$  and  $I_j(f)$  terms. The attenuation parameters ( $Q=62.5$ ) and velocity model were deduced from Bianco et al. (1999) and Scarpa et al. (2002), respectively. Thus, equation (1) can be rewritten as:

$$\frac{A_{ij}(f)}{P_{ij}(f) \cdot I_j(f)} = K_i(f) \cdot S_j(f) \quad (2)$$

$$\bar{A}_{ij}(f) = K_i(f) \cdot S_j(f) \quad (3)$$

where  $\bar{A}_{ij}$  is the first term of equation (2). The aim of this procedure is to evaluate the site term  $S_j(f)$  for each  $j$ th site. If we take the natural logarithm of equation (3), the expression becomes:

$$\ln(\bar{A}_{ij}(f)) = \ln(K_i(f)) + \ln(S_j(f)) \quad (4)$$

By considering the average of expression (4) evaluated on index  $i$ , by fixing the station-site index  $j$ , we obtain:

$$\langle \ln(\bar{A}_{ij}(f)) \rangle_i = \langle \ln(K_i(f)) \rangle_i + \ln(S_j(f)) \quad (5)$$

and the average evaluated on both indices  $i$  and  $j$  gives:

$$\langle \ln(\bar{A}_{ij}(f)) \rangle_{ij} = \langle \ln(K_i(f)) \rangle_i + \langle \ln(S_j(f)) \rangle_j \quad (6)$$

The term  $\langle \ln(S_j(f)) \rangle_j$  in expression (6) can be considered as the site-reference spectrum. In this case, we assume that this reference spectrum can be approximated by the spectrum averaged over the stations and earthquakes (Milana et al., 1996). The difference between expressions (6) and (5) gives the following formula:

$$\langle \ln(\bar{A}_{ij}(f)) \rangle_i - \langle \ln(\bar{A}_{ij}(f)) \rangle_{ij} = \ln(S_j(f)) - \langle \ln(S_j(f)) \rangle_j \quad (7)$$

By considering equation (7), it is possible to estimate the term  $S_j(f)$ , which describes the site effect of the  $j$ th site with respect to the average reference (Lachet et al., 1996; Del Pezzo et al., 1993). The use of local earthquakes with different focal mechanisms naturally averages the radiation pattern effects (Del Pezzo et al., 1993; Del Pezzo et al., 2004). In this study, the low magnitude of some of the selected seismic events did not allow the recording of good quality waveforms at all of the available seismic stations. A weighted average was used when we evaluated the first term of equation (5). The “weight” for the  $i$ th seismic event was considered the number  $n_i$  of station sites available for the  $i$ th seismic event.

### 3.2 Generalized Inversion

Equation (4) can be written for a fixed frequency as:

$$a_{ij}(f) = k_i(f) + s_j(f) \quad (8)$$

where  $a_{ij}(f)$  is the first term of equation (4),  $k_i(f)$  and  $s_j(f)$  are, respectively, the source and site-amplification terms of equation (4). Equation (8) can be expressed in a matrix form as (Bonilla et al., 1996):

$$\vec{d} = D \cdot \vec{m} \quad \forall f \quad (9)$$

where  $\mathbf{m}$  is the a vector in the model space, where the elements consist of  $k_i(f)$  and  $s_j(f)$ ,  $\mathbf{d}$  is the vector containing the amplitude  $a_{ij}(f)$ , and  $D$  is the matrix that relates  $\mathbf{m}$  to  $\mathbf{d}$ . Equation (9) can be resolved in the least square sense. This procedure is applied by constraining the summation of all of the site terms to unity (Hartzell, 1992). By considering this last assumption, equation (9) can be rewritten as:

$$\begin{bmatrix} \vec{d} \\ 0 \end{bmatrix} = \begin{bmatrix} D \\ F \end{bmatrix} \cdot \vec{m} \quad (10)$$

where  $\mathbf{F} \cdot \mathbf{m}$  is set to 0 to constrain the average site response to unity (Hartzell, 1992). Equation (10) can be rewritten in a more compact form as:

$$\vec{d}_c = \vec{D}_c \cdot \vec{m} \quad (11)$$

The solution for vector  $\mathbf{m}$  is given in the least square sense by (Lay and Wallace, 1995):

$$\vec{m}_{best} = \left( (D_c^T \cdot D_c)^{-1} \cdot D_c^T \right) \cdot \vec{d}_c \quad (12)$$

### 3.3 Coda Inversion

The time- and frequency-dependent amplitudes of the coda waves can be expressed as (Aki and Chouet, 1975):

$$A_{ij}(f,t) = K_i(f) \cdot S_j(f) \cdot I_j(f) \cdot C(f,t) \quad (13)$$

where  $A_{ij}(f,t)$  is the Fourier amplitude of the coda wave for the  $i$ th event recorded at the  $j$ th station for a lapse time  $t$ .  $C(f,t)$  is related to the coda decay curve and is expressed following the single back-scattering model, as (Aki and Chouet, 1975):

$$C(f,t) = (t^{-1}) \cdot \exp(-\pi ft / Qc) \quad (14)$$

where  $Qc$  is the quality factor of the coda waves. For the hypothesis of a common coda decay  $C(f,t)$  for all of the stations, equation (13) can be rewritten by taking the natural logarithm of each member. The resulting equation is solved by using the same procedure as for the inversion of the S-wave spectra, and the site-amplification terms  $S_j(f)$  are evaluated. By applying this method, we have used a lapse time  $t$  of 12 s and a window length of 6 s. This choice agrees with the need to set the lapse time  $t$  as three times the S-wave travel time of the furthest station used in the analysis (Margheriti et al., 1994). The value of  $Qc$  ( $Qc = 200$ ) for the Mt. Vesuvius area was taken from Bianco et al. (1999).

## 4. Results

The results obtained for the DSR, GI and CI methods are shown in Figures 2, 3 and 4, respectively.

Each panel in Figures 2, 3 and 4 shows the site-amplification function (bold black line) with errors (thin black lines) in the frequency band 1-25 Hz. As indicated above, the average spectrum was considered as the reference spectrum for the evaluation of the site-transfer function (DSR method). This assumption was equivalent to constraining the average spectra calculated over all of the site-amplification functions to unity (GI and CI methods). The results show that:

- the CDT station shows the highest amplification in the frequency range between 6 Hz and 10 Hz, and above 20 Hz (of 2 for the DSR method, and 3 for the GI and CI methods);
- the BKE and SGV site-response functions show a slight amplification, of 1.5 (DSR and GI methods) and 2.5 (CI method) in the frequency band of 6-18 Hz;
- BAF, BKN and SVT show a constant pattern of 1 in all of the frequency ranges;
- the POL transfer function shows a slight de-amplification (of 0.5) in the frequency range 1-25 Hz. The FTC site function shows de-amplification of around 0.5 above 10 Hz;
- The errors in the GI method results are greater at higher frequencies (above 10 Hz) than at lower ones. This was due to the greater contribution of uncertainties in the attenuation term at high frequencies.

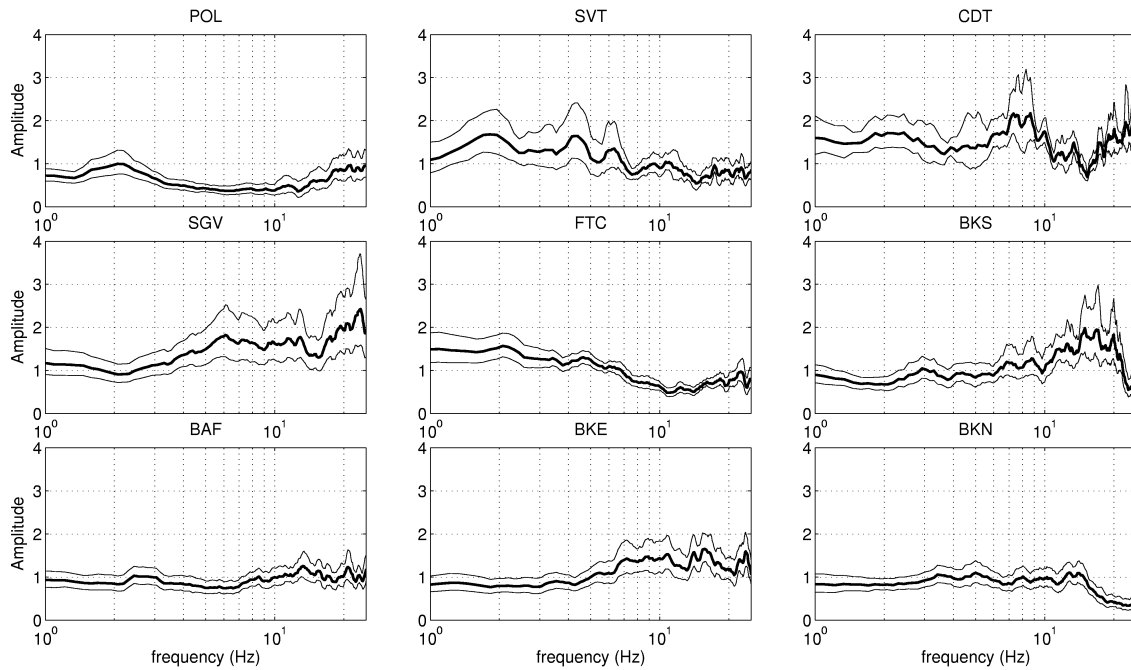


Figure 2 – Site responses calculated by the DSR method. The bold lines indicate site-response functions and thin lines indicate  $\pm$  one standard deviation of the result.

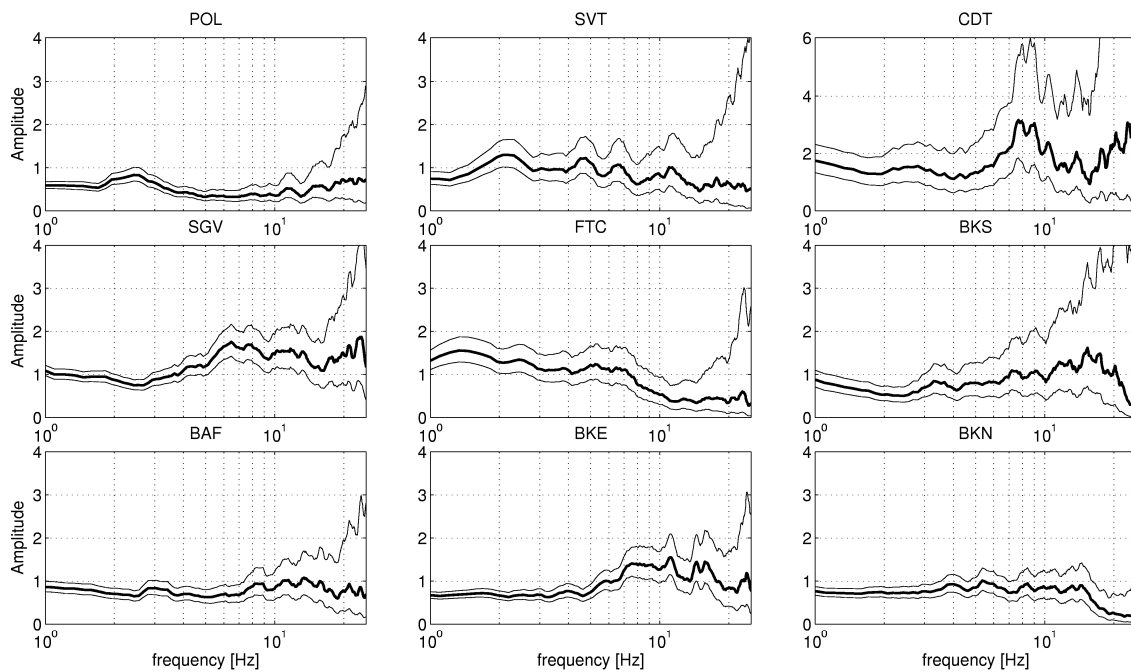


Figure 3 – Site responses calculated with the GI method.

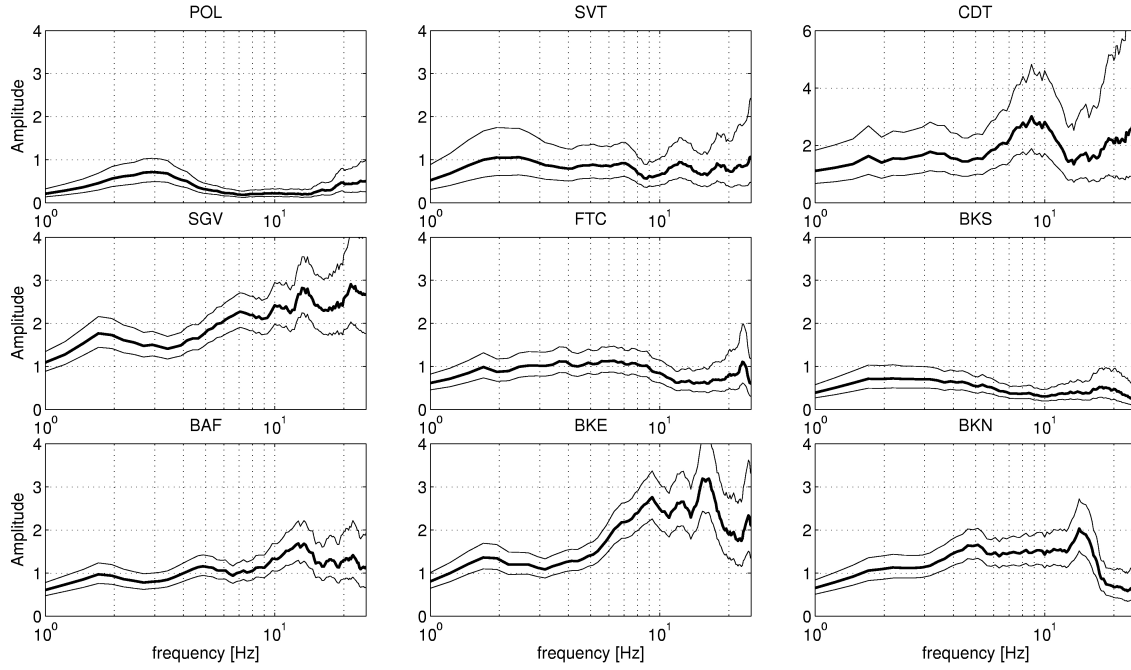


Figure 4 – Site responses calculated with the CI technique

The GI method gave the source velocity spectra for all of the selected earthquakes. The seismic moment, corner frequency, source radius and static stress drop were evaluated from the displacement spectra of direct S-waves corrected for instrument, site and attenuation terms. The seismic moment was estimated by considering the relation:

$$M_0 = \frac{4\pi\rho_0\beta_0^3 r\Omega_0}{2Y_{\theta\phi}} \quad (15)$$

where  $\Omega_0$ ,  $\beta_0$ ,  $\rho_0$  and  $Y_{\theta\phi}$  represent, respectively, the low frequency asymptote of the displacement spectrum, the velocity of the S wave at source, the density of the medium, and the radiation pattern term. The low frequency level was estimated by averaging the log-spectral amplitudes from 2 Hz to 8 Hz, while the high-frequency envelope was obtained by considering a linear fit of the log-spectral amplitudes in the frequency interval between 15 Hz and 25 Hz. The corner frequency was calculated by the intersection of the low frequency asymptote with the high frequency envelope, as described in Del Pezzo et al. (2004). The source radii were evaluated by considering the relation (Brune, 1970):

$$r = 0.37 \cdot \frac{\beta_0}{f_c} \quad (16)$$

The pattern of the seismic moment,  $M_0$ , versus the source radii,  $r$ , is plotted in Figure 5.

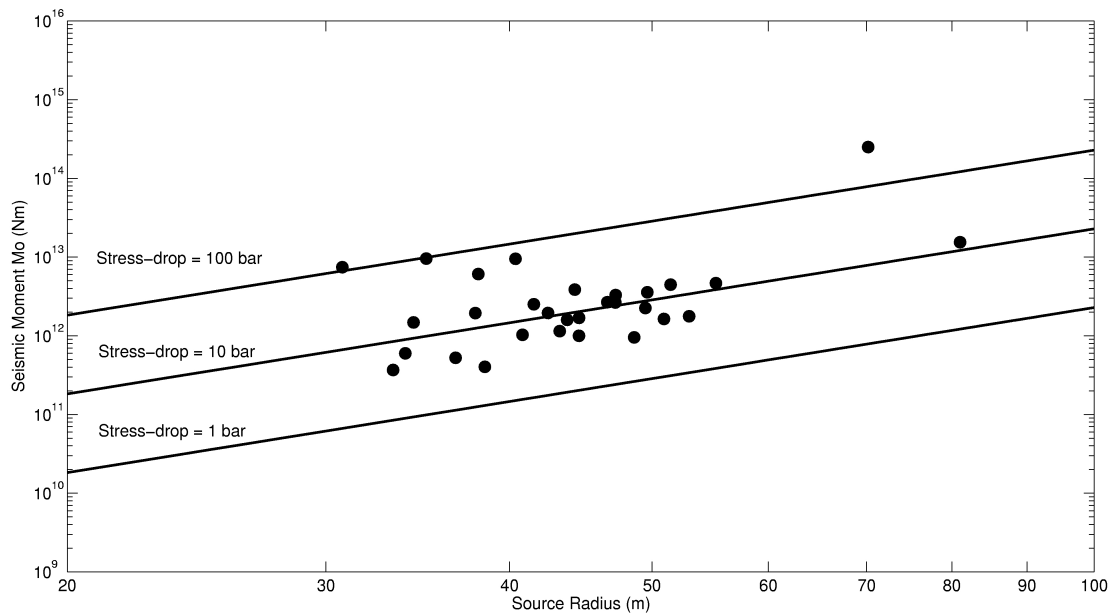


Figure 5 – Seismic moment as a function of Brune's source radius. Lines of equal stress drops (1, 10, 100 bar) are also shown.

The lines of equal stress drop (1, 10 and 100 bar) are also plotted in Figure 5. The results show that the selected earthquakes are characterized by a stress-drop distribution around 10 bar. This result is similar to the scaling law of local earthquakes found for the area of Campi Flegrei, which is located close to Mt. Vesuvius. In the case of Campi Flegrei, the source dimensions and seismic moments are confined by the 1 bar to 10 bar constant stress-drop lines (Del Pezzo et al., 1987).

## 5. Conclusions

Site-amplification factors obtained for the area under investigation showed similar results when comparing the DSR, GI and CI methods. The first two of these use direct S-wave window spectra, with the assumption that the azimuth effects are negligible and the radiation pattern effects are minimized by averaging over earthquakes with different fault-plane solutions.

Stations BKE and SGV showed a nearly constant pattern (equal to unity) in the frequency band of 1-6 Hz. The same stations showed amplification factors near to 1.5 (DSR and GI methods) or equal to 2.5 (CI method) in the frequency band of 6-18 Hz. The CDT peak frequency (8 Hz) and the amplification values (of 3 for the GI and CI methods, and 2 for DSR) are similar across all three of the methods.

The uncertainty associated with the estimates evaluated by these three methods are strongly dependent on the uncertainty of the input parameters. This is shown clearly by the GI method results.

Site-corrected source displacement spectra were used to evaluate the spectral parameters of the seismic source, including the seismic moment,  $M_0$ , and the corner frequency. With the hypothesis of circular cracks for the seismic sources, the source radii,  $r$ , were evaluated. The pattern of the seismic moment  $M_0$  versus the source dimension  $r$  showed a constant stress-drop distribution around 10 bar. This last result highlights the



importance of separating the path and site terms from the amplitude spectra to obtain more precise information about the source characteristics. Future developments will be addressed to the estimation of site effects with the H/V spectral ratio technique applied to the S-wave window and to the seismic ambient noise, as has been indicated in other studies reported in the literature (Field and Jacob, 1995). Furthermore, a more accurate investigation will be necessary to correctly correlate the evaluated site effects with the surface unconsolidated deposits, or with a topographical site effect generated by the shape of the Mt. Vesuvius volcanic complex.

## 6. References

- Aki, K. and B. Chouet (1975). Origin of coda waves: source, attenuation and scattering effect. *Journal of Geophysical Research* 80, 3322-3342.
- Bonilla, L. F., H. J. Steidl, G. T. Lindley, A. G. Tumarkin and R. Archuleta (1997). Site amplification in the San Fernando Valley, California: Variability of the Site effect Estimation Using the S-Wave, Coda and H/V methods. *Bulletin of Seismological Society of America* 87 (3), 710-730.
- Bianco, F., M. Castellano, E. Del Pezzo and J. M. Ibanez (1999). Attenuation of short period seismic waves at Mt. Vesuvius, Italy. *Geophysical Journal International* 138, 67-76.
- Borcherdt, R. D. (1970). Effects of local geology on ground motion near San Francisco Bay. *Bulletin of Seismological Society of America* 60, 29-61.
- Brune, J. N. (1970). Tectonic stress and seismic shear waves from earthquakes. *Journal of Geophysical Research* 75, 4997-5009.
- Del Pezzo, E., G. De Natale, M. Martini, A. Zollo (1987). Source parameters of microearthquakes at Phlegraean Fields (Southern Italy) volcanic area. *Physics of the Earth and Planetary Interiors* 47, 25-42.
- Del Pezzo, E., S. De Martino, M.T. Parrinello, C. Sabbarese (1993). Seismic site amplification factors in Campi Flegrei, Southern Italy. *Physics of the Earth and Planetary Interiors* 78, 105-117.
- Del Pezzo, E., F. Bianco, G. Saccorotti (2004). Seismic source dynamics at Vesuvius volcano, Italy. *Journal of Volcanology and Geothermal Research* 133, 23-39.
- Drouet, S., A. Souriau, F. Cotton (2005). Attenuation, Seismic Moments and Site Effects for Weak Motion Events: Application to Pyrenees. *Bulletin of Seismological Society of America* 95 (5), 1731-1748.
- Field, E. H., K. H. Jacob (1995). A comparison and test at various site-response estimation techniques including three that are not reference site-dependent. *Bulletin of Seismological Society of America* 85, 1127-1143.
- Hartzell, S. H. (1992). Site Response Estimation from Earthquake Data. *Bulletin of Seismological Society of America* 82 (6), 2308-2327.
- Jin, A., C.A. Moya, M. Ando (2000). Simultaneous Determination of Site Response and Source parameters of Small Earthquakes along the Atotsugawa Fault Zone, Central Japan. *Bulletin of Seismological Society of America*, 90 (6), 1430-1445.
- Lachet, C., D. Hatzfeld, P. Bard, N. Theodulidis, C. Papaioannou and A. Savvaidis (1996). Site Effect and Microzonation in the City of Thessaloniky (Greece). Comparison of Different Approaches. *Bulletin of Seismological Society of America* 86 (6), 1692-1703.
- Lay, T., and T. C. Wallace. *Modern Global Seismology*. Academic Cambridge Press, London, 1995.

Margheriti, L., L. Wennerberg, J. Boatwright (1994). A comparison of coda and S-wave spectral ratio estimates of site response in the southern San Francisco Bay area. *Bulletin of Seismological Society of America* 84, 1815-1830.

Milana, G., S. Barba, E. Del Pezzo, E. Zambonelli (1996). Site response from ambient noise measurements: new perspectives from an array study in central Italy. *Bulletin of Seismological Society of America* 86, 320-328.

Parolai, S., D. Bindi, L. Troiani (2001). Site response for the RSM Seismic Network and Source Parameters in the Central Appenines (Italy). *Pure and Applied Geophysics* 158, 695-715.

Scarpa, R., F. Tronca, F. Bianco, E. Del Pezzo (2002). High Resolution velocity structure beneath Mount Vesuvius from seismic array data. *Geophysics Research Letters* 29, 2040.

Tsujura, M. (1978). Spectral analysis of coda waves from local earthquakes. *Bulletin Earthquake Research Institute, Tokyo University*, 53, 1-48.